

A Raman scattering investigation of the magnetic ordering in the two-dimensional triangular lattice antiferromagnet LiCrO_2

This article has been downloaded from IOPscience. Please scroll down to see the full text article.

1993 J. Phys.: Condens. Matter 5 4225

(<http://iopscience.iop.org/0953-8984/5/25/012>)

View [the table of contents for this issue](#), or go to the [journal homepage](#) for more

Download details:

IP Address: 171.66.16.96

The article was downloaded on 11/05/2010 at 01:25

Please note that [terms and conditions apply](#).

A Raman scattering investigation of the magnetic ordering in the two-dimensional triangular lattice antiferromagnet LiCrO_2

M Suzuki†, I Yamada†, H Kadowaki‡ and F Takei‡

† Department of Physics, Faculty of Science, Chiba University, Yayoi-cho, Inage-ku, Chiba 263, Japan

‡ Institute for Solid State Physics, The University of Tokyo, Roppongi, Minato-ku, Tokyo 106, Japan

Received 22 January 1993, in final form 16 March 1993

Abstract. Raman scattering experiments were performed on the two-dimensional triangular lattice antiferromagnet LiCrO_2 to investigate its magnetic ordering. Besides two phonon lines which are assigned to the E_g and the A_{1g} modes of D_{3d} point symmetry, additional lines having broader linewidth than that of the phonon lines are observed at low temperatures. Their intensity becomes weak with increasing temperature, but they are still observable above $T_N = 62$ K, a value that was determined by neutron diffraction experiments, and only become unobservable at around 150 K. The lines are found to correspond to two-magnon lines when a 120° Néel structure is assumed. A possible effect of the Z_2 vortex on two-magnon lines in a two-dimensional triangular lattice Heisenberg antiferromagnet is discussed.

1. Introduction

Triangular lattice antiferromagnets (TALAFs) have recently attracted much attention because they show the possibility of exhibiting magnetic ordering which is against the Néel state. The compound LiCrO_2 is a candidate for a Heisenberg TALAF. It belongs to the family of AMO_2 (A is an alkali metal and M a 3d metal), which crystallize in the layer structure of the space group D_{3d}^5 (or $R\bar{3}m$). Its crystal structure is shown in figure 1. No crystallographic phase transition occurs below 400°C as has been confirmed by Hewston and Chamberland [1]. Since the triangular lattice sheets which involve the magnetic ions Cr^{3+} with $S = 3/2$ are separated by the two layers of Li^+ and O^{2-} , its magnetic two-dimensionality should be excellent. Although several investigations of the magnetic properties of LiCrO_2 have been made, its magnetic ordered structure is not known definitely as yet. The susceptibility measured by Delmas *et al* [2] shows a cusp-like peak around 75 K and yields the Weiss temperature $\theta = -680$ K, indicating its excellent two-dimensionality. Analysing the susceptibility on the basis of a Heisenberg Rushbrook–Wood model, they deduced the exchange interaction in the Heisenberg Hamiltonian $-2J \sum_{ij} S_i \cdot S_j$ as $J = -39 \pm 1$ K. The two-dimensionality of this compound has also been confirmed by a Mössbauer study [3].

Although the susceptibility did not show a clear-cut phase transition in its temperature dependence, the neutron diffraction pattern obtained by Soubeyroux *et al* [4] showed a decrease of the intensity of the magnetic Bragg peak until 62 K and only a broad diffuse bump was observed above this temperature. From this result, $T_N = 62$ K was determined.

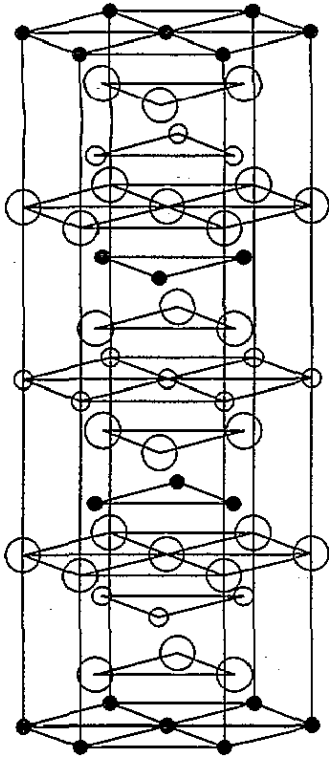


Figure 1. Crystal structure of LiCrO_2 . Large open circles are O, small open circles are Li and filled circles are Cr.

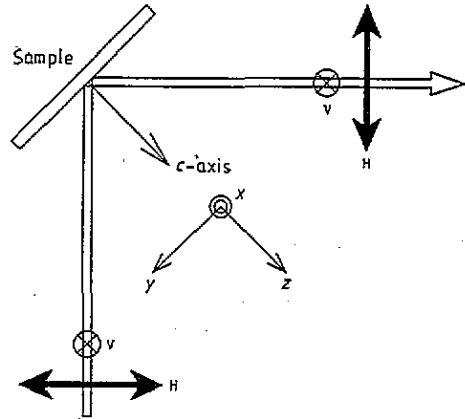


Figure 2. Experimental geometry of the polarization of the incident and scattered light with respect to the crystal axis. H (horizontal) and v (vertical) indicate the direction of the polarization of the incident and scattered light.

They proposed several models for the ordered spin structure and compared them with the experimental result. None of them, however, gave reasonable agreement with the observed intensities of the magnetic Bragg peaks. They subsequently performed neutron diffraction experiments [5] on a single crystal and suggested a 120° spin structure.

On the other hand, Ajiro *et al* [6] carried out EPR experiments on this compound. Their EPR absorption line shows an anomaly at 65 ± 2 K which coincides well with $T_N = 62$ K determined by neutron diffraction. Their motivation is to investigate the effect of the dissociation of the Z_2 vortex which is expected in a TALAF as theoretically shown by Kawamura and Miyashita (KM) [7].

Taking these results into consideration, we performed Raman scattering experiments over the temperature range of ~ 14 – 300 K to investigate the magnetic structure.

2. Experimental procedure and results

Raman measurements were performed with a laboratory-assembled instrument consisting of a monochromator, a cooled photomultiplier, and a photon counter, with several optical elements and interfaced with a personal computer for data acquisition. A 514.5 nm polarized line of an argon laser with a power of 50 mW was employed as a light source, the power of

which was low enough to prevent self-heating of the sample. To attain low temperatures, we used a closed-cycle refrigerator. The sample used was a single crystal of size $2 \times 2 \times 0.2 \text{ mm}^3$. Because of its small size along the c axis and dark-green colour, we were obliged to employ a back-scattering geometry instead of a 90° one. To reduce the tail of the Rayleigh line, the polarization measurements were made under a geometry shown in figure 2 in which the laboratory coordinates (x, y, z) are also shown. That is, light is incident at 45° on a surface perpendicular to the c axis and scattered light coming out at 90° to the direction of the incident light is collected. The polarization of both the incident and scattered light is either vertical (V) or horizontal (H). There are therefore four choices, VV, VH = HV and HH for the polarizations of the incident and scattered light. The geometry of HH, for instance, contains the configurations of yy and zz . We show the polarized spectrum in figure 3 for HH. This spectrum consists of the overlapping of yy and zz . Figure 4 is an overlapped spectrum of xy and xz , taken under the condition of VH. Two strong lines denoted as P_1 and P_2 in both spectra were observed over the whole range of $\sim 14\text{--}300 \text{ K}$.

Besides these two lines, an additional broad line named the M line appears at low temperatures as can be seen in figures 3 and 4. Its peak position is approximately at $350\text{--}360 \text{ cm}^{-1}$. This line becomes weak with increasing temperature and is so weak above 150 K as to be impossible to distinguish from the noisy base line. It remains, however, above $T_N = 62 \text{ K}$. This temperature behaviour strongly suggests that the line has a magnetic origin. Furthermore a swelling is found on the wings of the P_2 line as indicated by arrows in both figures 3 and 4. Since the swelling disappears gradually with increasing temperature, we think that it is probably the tail of a magnetic line having its peak around $550\text{--}580 \text{ cm}^{-1}$, the main part of which is hidden by the phonon line P_2 .

3. Discussion

The two strong lines, P_1 and P_2 , are reasonably attributed to phonon scattering. The P_2 line appearing in figure 4 is a leakage of the line appearing at the same position in figure 3, which we confirmed by rotating the analyser from H to V. As the factor group analysis for the D_{3d} point symmetry shows [8], two phonon modes, E_g and A_{1g} , are expected in the present case. The E_g mode is a vibration of O atoms perpendicular to the c axis and its phonon line should appear in the xx , xy and xz spectra. The A_{1g} mode is, on the other hand, a vibration of O atoms parallel to the c axis and should be detected as a phonon line in the xx and zz spectra. Furthermore the energy of the A_{1g} mode is higher than that of the E_g mode, as predicted by the harmonic oscillator model [9]. The P_1 line is therefore the E_g mode and the P_2 line the A_{1g} mode.

We now discuss the magnetic line observed at $350\text{--}360 \text{ cm}^{-1}$. Since the magnetic anisotropy of this compound is very weak, as the g value obtained by ESR measurements [10] suggests, the energy of the spin wave at the zone centre should be less than several cm^{-1} . The intensity of the one-magnon line of such a Heisenberg system should be very weak because it is proportional to $(H_A/H_E)^{1/2}$ [11] where H_A and H_E indicate the anisotropy field and the exchange field, respectively. Moreover, the renormalization of the zone-centre magnons is like that of $\langle S_z \rangle$ and therefore the one-magnon line, if its intensity is strong enough to be observed, should disappear above T_N . From these facts, the one-magnon process is out of the question in the present case. Thus we base our examination of the magnetic lines on a two-magnon process. We first derive the dispersion relations restricting the exchange interactions only among the nearest-neighbour spins in the c plane and setting

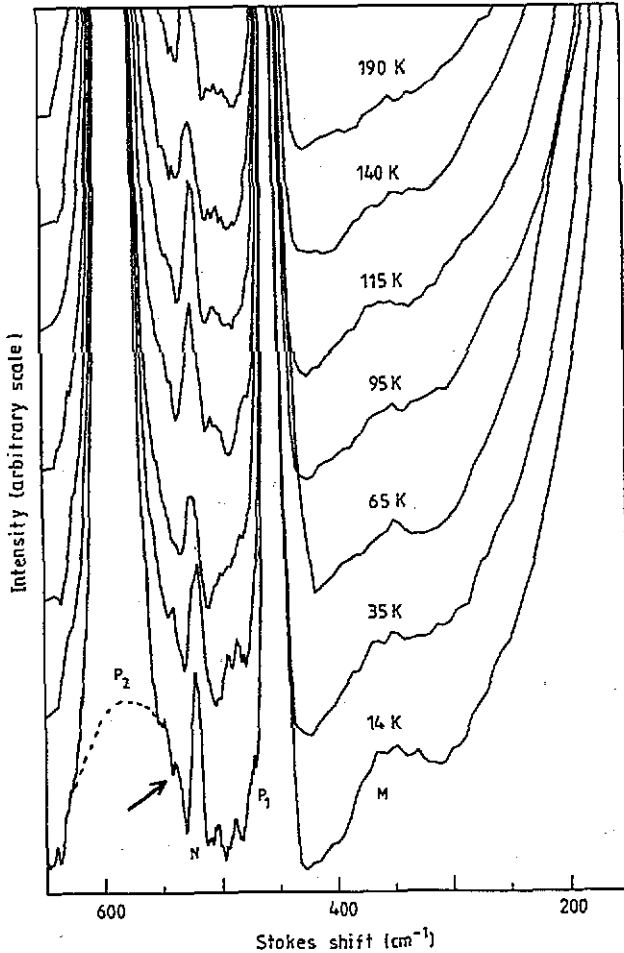


Figure 3. Polarized Raman spectra taken under the condition HH of the polarization of the incident and scattered light. The $xx = yy$ and zz configurations are then overlapped in these spectra. The lines P_1 and P_2 correspond to the phonon modes of the E_g and the A_{1g} , respectively and the M line at $350\text{--}360\text{ cm}^{-1}$ is a magnetic one. The swelling indicated by an arrow is probably the tail of another magnetic line (broken curve), the peak of which is around $550\text{--}580\text{ cm}^{-1}$ but is hidden by the strong P_2 line. A peak indicated by N is a natural line.

the spins on three sublattices at 120° to each other. The Hamiltonian is then given by

$$\mathcal{H} = -2J \sum_{i>j} \mathbf{S}_i \cdot \mathbf{S}_j \quad \text{with} \quad J < 0. \quad (1)$$

Since the interlayer exchange interaction and the magnetic anisotropy are very small, no serious problem arises for the zone-edge magnon energies if we neglect them. With reference to the method developed by Oguchi [12], three branches of the magnon energies are obtained as

$$\begin{aligned} \hbar\omega_1 &= 2|J|S\{[3 + 2\Phi_k(0)][3 - \Phi_k(0)]\}^{1/2} \\ \hbar\omega_2 &= 2|J|S\{[3 + 2\Phi_k(-2\pi/3)][3 - \Phi_k(-2\pi/3)]\}^{1/2} \\ \hbar\omega_3 &= 2|J|S\{[3 + 2\Phi_k(2\pi/3)][3 - \Phi_k(2\pi/3)]\}^{1/2} \end{aligned} \quad (2)$$

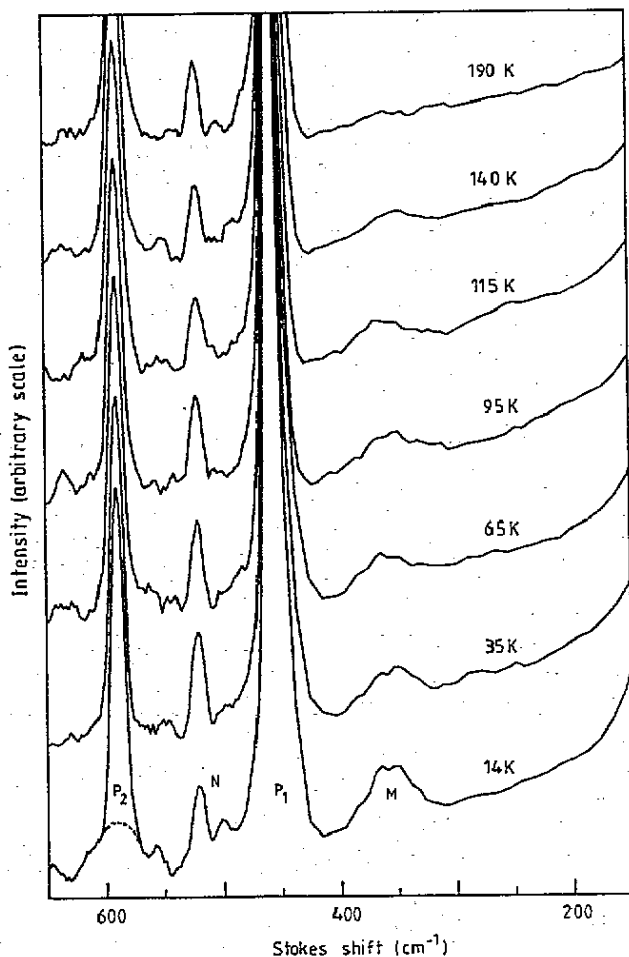


Figure 4. Polarized Raman spectra taken under the condition ν_H . The $xy = yx$ and $xz = zx$ spectra are overlapped. P_1 and P_2 are the phonon lines and M the magnetic one as explained in the caption of figure 3. The hidden magnetic line is indicated by the broken curve.

where

$$\Phi_k(\theta) = \cos[2\pi(h-k)/3 + \theta] + \cos[2\pi(h+2k)/3 + \theta] + \cos[-2\pi(2h+k)/3 + \theta]$$

and (hkl) indicates the components of the wave vector k . The three branches thus obtained are shown in figure 5. The energies of the ω_1 and the ω_2 modes at the zone boundary degenerate. The magnon density of states calculated from equations (2) shows two peaks at $\hbar\omega/2|J|S = 3.16$ and 2.00 which correspond to the energies at the zone boundary. Introduction of an interlayer exchange interaction, if its value is very small as in the present case, does not bring about much change of the zone-edge energies.

We next calculate the spin-dependent polarizability α of spin pairs following the conventional method given by Moriya [13]. For the two-magnon process, only the bilinear terms in the spin components are effective in α and we express it as

$$\alpha = \sum_{i>j} \alpha_{ij} S_i \cdot S_j. \quad (3)$$

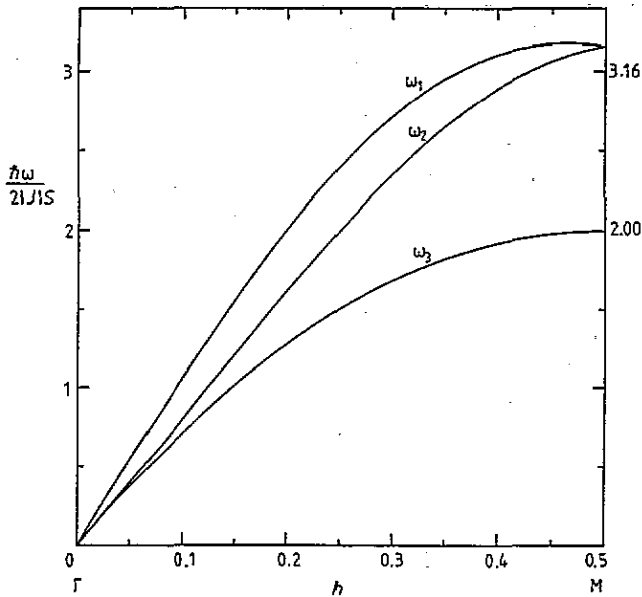


Figure 5. Calculated dispersion relations reduced to the Γ -M line.

As the theory [13] shows, the crystal symmetry around the pairs of ions i and j are relevant to α_{ij} . A concrete derivation of α_{ij} for the spins on the triangular lattice is developed in [8] and here we merely show the final expression of it. The bilinear terms which create two-magnon scattering are given by

$$\alpha = \sum_k \mathbf{S}_k \cdot \mathbf{S}_{-k} \left\{ \begin{pmatrix} -a_1 & & \\ & a_1 & a_2 \\ & a_2 & \end{pmatrix} \Gamma_1(k) + \begin{pmatrix} & a_1 & -a_2 \\ a_1 & & \\ -a_2 & & \end{pmatrix} \Gamma_2(k) \right\} \quad (4)$$

where

$$\Gamma_1(k) = \frac{1}{2} \{ 2 \cos[2\pi(h-k)/3] - \cos[2\pi(2h+k)/3] - \cos[2\pi(h+2k)/3] \}$$

and

$$\Gamma_2(k) = (\sqrt{3}/2) \{ \cos[2\pi(2h+k)/3] - \cos[2\pi(h+2k)/3] \}.$$

Both $\Gamma_1(k)$ and $\Gamma_2(k)$ have their maximum values at the M point and its equivalents. As theories of light scattering indicate, the scattering intensity is approximately proportional to α^2 . Since this value is extremely large at the M point, it is these magnons that play a dominant role in the two-magnon scattering. From these results, two two-magnon lines as Stokes lines are expected at the energies of

$$\hbar\omega = \begin{cases} 4|J|S \times 3.16 \\ 4|J|S \times 2.00. \end{cases} \quad (5)$$

The matrices in equation (4) also indicate the configurations of polarization of the incident and scattered light which can produce the two-magnon scattering. We find that the $xx(=yy)$, $xy(=yx)$ and $xz(=zx)$ spectra will show two-magnon lines.

Based on the theory developed above, we analyse the experimental results. As can be seen in figures 3 and 4, the M line and the hidden line appear in the spectrum containing the configurations of polarization of xx , zz and zx , which agrees with the theoretical prediction. When $J = -39$ K as proposed in [4] and $S = 3/2$ are introduced in equation (5), the two-magnon lines should appear at 514 cm^{-1} and 325 cm^{-1} , which nearly coincide with the positions of the hidden line and the M line, respectively. In contrast with the discussion above, $J = -42 \pm 1$ K is obtained when the energies of the hidden and M lines are applied to equation (5). This value approximately agrees with that in [4]. As a consequence the M line and the hidden line surely correspond to the two-magnon lines of the 120° spin structure.

We finally refer to a possible effect of Z_2 vortices on two-magnon lines. As the theory [7] shows, a two-dimensional TALAF with only the nearest-neighbour Heisenberg exchange interaction has a topologically stable point defect known as Z_2 vortices. The dissociation of paired vortices causes a new type of phase transition at a temperature given by $T_{\text{KM}} = 0.66|J|S^2$.

When $J = -39 \pm 1$ K, as pointed out in [6], $T_{\text{KM}} \simeq 56\text{--}59$ K is calculated. This value is very close to $T_{\text{N}} = 62$ K determined in [4]. This fact, according to [6], suggests that LiCrO_2 inheres in the Z_2 vortex, although the three-dimensional ordering at $T_{\text{N}} = 62$ K is triggered by an unavoidable interlayer coupling or a small Ising-type anisotropy. From this point of view, the dependence of the EPR linewidth of this compound on temperature was analysed [6]. The EPR linewidth of an ordinary low-dimensional Heisenberg antiferromagnet increases gradually with decreasing temperature over the short-range-order area. The present compound, as well as VCl_2 , another candidate for the Z_2 vortex system, shows a very weak increase of the EPR linewidth over the short-range-order region; rapid increase of the linewidth rather appears over a narrow temperature range above T_{N} in spite of the excellent two-dimensionality of these compounds. Such an unusual phenomenon is thought to be caused by the growing of the Z_2 vortices.

We think that the magnetic lines observed in LiCrO_2 should be examined from the same viewpoint. Various experiments and theories of two-magnon light scattering have revealed that a two-magnon line persists in the paramagnetic regime. This is because the zone-edge magnon pairs renormalize more slowly than do the zone-centre magnons. The intensity of two-magnon lines observed in ordinary three-dimensional antiferromagnets such as MnF_2 [14], NiF_2 [15], KNiF_3 [16] and so on seems to increase rather than decrease above T_{N} , but eventually the linewidth becomes too wide to be distinguishable from the baseline, so that the two-magnon line seems to disappear above a certain temperature far above T_{N} . The renormalization in low-dimensional antiferromagnets should be smaller, as confirmed for K_2NiF_4 [17].

Since the two-magnon lines observed in the present experiments are not well shaped, it is impossible to trace them quantitatively above T_{N} . It seems, however, that the intensity decreases continuously with increasing temperature but persists above T_{N} . Besides LiCrO_2 , the compound VCl_2 , which is another candidate for the Z_2 vortex system as mentioned before, also shows a rapid decrease of the intensity of the two-magnon lines, as reported recently [8]. We cannot, however, insist that the decreasing rate of the intensity observed in these two triangular systems is completely different from that observed in the ordinary antiferromagnets introduced above.

Spontaneous generation of the vortices above T_{N} should influence the fluctuation of spins having the zone-edge wavevector and probably produces a temperature dependence of the two-magnon lines different from that observed in the ordinary antiferromagnets introduced above. This point should be clarified theoretically.

In conclusion, the present Raman study revealed a 120° structure of LiCrO_2 . Further theoretical studies concerning the effect of the Z_2 vortex on renormalization of the zone-edge magnon pairs in a two-dimensional Heisenberg TALAF are anticipated.

Acknowledgments

Thanks are due to H Onda for his help in experiments. This study was partly supported by a grant from Fujitsu Ltd.

References

- [1] Hewston T A and Chamberland B L 1987 *J. Phys. Chem. Solids* **48** 97
- [2] Delmas C, Le Flem G, Fouassier C and Hagenmuller P 1978 *J. Phys. Chem. Solids* **39** 55
- [3] Delmas C, Menil F, Le Flem G, Fouassier C and Hagenmuller P 1978 *J. Phys. Chem. Solids* **39** 51
- [4] Soubeyroux J L, Fruchart D, Delmas C and Le Flem G 1979 *J. Magn. Magn. Mater.* **14** 159
- [5] Soubeyroux J L, Fruchart D, Marmeggi J C, Fitzgerard W J, Delmas C and Le Flem G 1981 *Phys. Status Solidi a* **67** 633
- [6] Ajiro Y, Kikuchi H, Sugiyama S, Nakashima T, Shamoto S, Nakayama N, Kiyama M, Yamamoto N and Oka Y 1988 *J. Phys. Soc. Japan* **57** 2268
- [7] Kawamura H and Miyashita S 1984 *J. Phys. Soc. Japan* **53** 4138
- [8] Sugawara K and Yamada I 1993 *J. Phys.: Condens. Matter* **5** 1427
- [9] Frey Th and Benedek G 1979 *Solid State Commun.* **32** 305
- [10] Angelov S, Darriet J, Delmas C and Le Flem G 1984 *Solid State Commun.* **50** 345
- [11] Fleury P A and Loudon R 1968 *Phys. Rev.* **166** 514
- [12] Oguchi T 1983 *J. Phys. Soc. Japan Suppl.* **52** 183
- [13] Moriya T 1967 *J. Phys. Soc. Japan* **23** 490
- [14] Brya W J and Richards P M 1974 *Phys. Rev. B* **39** 2244
- [15] Brya W J, Richards P M and Fleury P A 1973 *AIP Conf. Proc.* **10** 729
- [16] Balucani U and Tognetti V 1977 *Phys. Rev. B* **16** 271
- [17] Fleury P A and Guggenheim H J 1970 *Phys. Rev. Lett.* **24** 1346